

Intramolecular activation of aromatic C–H bonds at tantalum(v) metal centers: evaluating cyclometallation ‘resistant’ and ‘immune’ aryloxide ligation†

Jonathan S. Vilardo, Mark A. Lockwood, Linda G. Hanson, Janet R. Clark,
Bernardeta C. Parkin, Phillip E. Fanwick and Ian P. Rothwell*

Department of Chemistry, 1393 Brown Building, Purdue University, West Lafayette, IN 47907-1393, USA

The trichloride compounds $[\text{Ta}(\text{OC}_6\text{HPh}_2\text{-2,6-R}_2\text{-3,5})\text{Cl}_3]$ (**1**: R = H **a**, Ph **b**, Me **c**, Prⁱ **d** or Bu^t **e**) have been obtained by treating $[\text{Ta}_2\text{Cl}_{10}]$ with the corresponding 3,5-disubstituted-2,6-diphenylphenols **1a–1e**. The solid-state structures of **1c** and **1d** show a square-pyramidal structure with an axial aryloxide ligand. The reaction of **1** with $\text{LiCH}_2\text{SiMe}_3$ (3 equivalents) led to the isolation of the tris(alkyls) $[\text{Ta}(\text{OC}_6\text{HPh}_2\text{-2,6-R}_2\text{-3,5})_2(\text{CH}_2\text{SiMe}_3)_3]$ (**4a–4d**) except in the case of the 3,5-di-*tert*-butyl derivative **1e** which generated the alkylidene compound $[\text{Ta}(\text{OC}_6\text{H}_3\text{Ph}_2\text{-2,6-Bu}^t\text{-3,5})_2(=\text{CHSiMe}_3)(\text{CH}_2\text{SiMe}_3)]$ **6e**. The alkylidenes **6a–6d** can be produced by photolysis of the corresponding tris(alkyls) **4a–4d**. The alkylidenes **6a–6d** undergo intramolecular cyclometallation of the aryloxide ligand (addition of an aromatic C–H bond to the tantalum alkylidene) at a rate which is extremely dependent on the *meta* substituents on the phenoxide nucleus. Kinetic studies show that conversion of **6a–6d** into mono-metallated **7a–7d** is first order with the phenyl, methyl and isopropyl substituents slowing the ring closure down by factors of 20, 90 and 360 respectively. The *tert*-butyl substituent completely shuts down cyclometallation of the adjacent phenyl ring. It is argued that bulky substituents inhibit rotation of the *ortho*-phenyl ring into a conformation necessary for C–H bond activation. Structural analysis of the torsion angles between *ortho*-phenyl and phenoxy rings has been carried out. The use of ^1H NMR chemical shifts has been demonstrated to be a valuable tool to probe the average conformations adopted in solution.

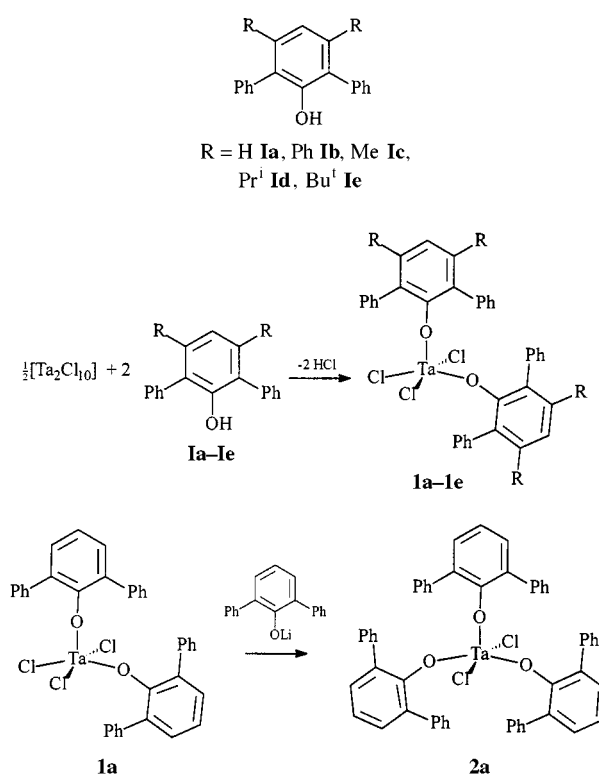
The use of sterically demanding ligation has made impacts in many areas of inorganic and organometallic chemistry.¹ A recurring problem with the design of bulky ligands to stabilize highly reactive species is the sometimes facile, intramolecular activation of C–H bonds within the ligand itself.² In the case of aryloxide ligation, cyclometallation reactions have led not only to the isolation of a variety of oxa-metallacycle rings^{3,4} but also in some cases to the overall dehydrogenation of substituent alkyl groups.⁵ Having spent considerable effort to understand the mechanistic pathways whereby cyclometallation of aryloxide ligands occurred, we set out to design a new generation of more metallation resistant, bulky aryloxide ligands.

The cyclometallation of 2,6-diphenylphenoxide ligands (**1**) occurs readily at electrophilic main-group-metal centers⁶ as well as with a variety of high- and low-valent d-block metal systems.⁷ Recognizing that rotation of the *ortho*-phenyl ring almost coplanar with the central phenoxide core is necessary for C–H bond activation led to the simple notion that the introduction of *meta* substituents should impede the cyclometallation.⁸ This paper details experiments in which intramolecular activation of aromatic C–H bonds of 2,6-diphenylphenoxides (*meta*-Ph **1b**, Me **1c**, Prⁱ **1d** or Bu^t **1e**) by tantalum alkylidene functional groups is indeed controlled by the nature of *meta* substituents. These experiments show that the ligand 2,6-diphenyl-3,5-di-*tert*-butylphenoxide (first synthesized by Barton and co-workers)⁹ is inert towards cyclometallation in this system and leads to a thermally stable tantalum alkylidene derivative.^{10,11}

Results and Discussion

Synthesis and characterization of compounds

The reaction of $[\text{Ta}_2\text{Cl}_{10}]$ with the 3,5-disubstituted-2,6-diphenyl-



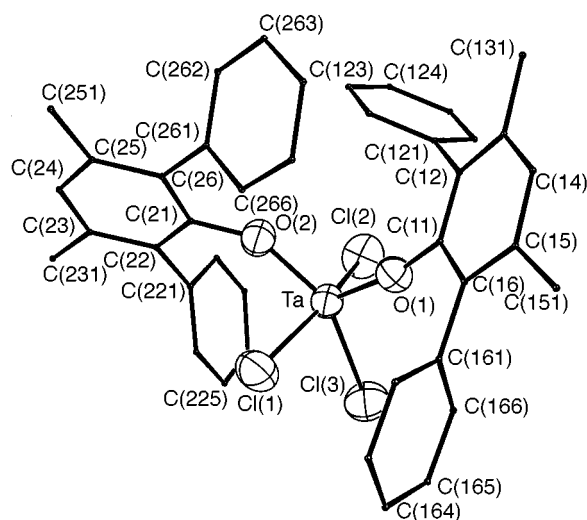
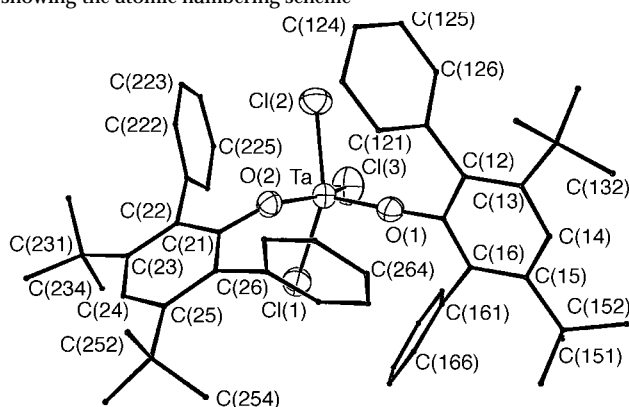
Scheme 1 R = H **a**, Ph **b**, Me **c**, Prⁱ **d** or Bu^t **e**

phenols ($\text{HOC}_6\text{HPh}_2\text{-2,6-R}_2\text{-3,5}$; R = H **1a**, Ph **1b**, Me **1c**, Prⁱ **1d** or Bu^t **1e**) in hydrocarbon solvents leads to formation of the bright yellow bis(aryloxides) **1** in good yield (Scheme 1). The solid-state structures of **1c** and **1e** show a square-pyramidal geometry for the mononuclear compounds with an axial aryloxide ligand (Table 1, Figs. 1 and 2). These molecules are

† Dedicated to the Memory of Professor Sir Geoffrey Wilkinson.

Table 1 Selected bond distances (Å) and angles (°) for [Ta(OC₆HPh₂-2,6-R₂-3,5)₂Cl₃] (R = Me **1c** or Bu^t **1e**)

	1c	1e
Ta–O(1)	1.803(3)	1.810(2)
Ta–O(2)	1.862(3)	1.883(2)
Ta–Cl(1)	2.358(1)	2.3348(9)
Ta–Cl(2)	2.308(1)	2.3092(9)
Ta–Cl(3)	2.347(1)	2.3430(9)
Cl(1)–Ta–Cl(2)	158.09(5)	153.63(4)
Cl(1)–Ta–Cl(3)	85.25(5)	85.08(4)
Cl(1)–Ta–O(1)	100.66(9)	102.40(7)
Cl(1)–Ta–O(2)	85.08(10)	84.31(7)
Cl(2)–Ta–Cl(3)	86.53(5)	87.06(4)
Cl(2)–Ta–O(1)	100.99(9)	103.86(7)
Cl(2)–Ta–O(2)	92.1(1)	90.98(7)
Cl(3)–Ta–O(1)	103.31(9)	102.15(7)
Cl(3)–Ta–O(2)	150.37(9)	151.81(7)
O(1)–Ta–O(2)	106.0(1)	105.61(9)
Ta–O(1)–C(11)	168.4(3)	178.3(2)
Ta–O(2)–C(21)	151.1(3)	140.9(2)

**Fig. 1** Molecular structure of [Ta(OC₆HPh₂-2,6-Me₂-3,5)₂Cl₃] **1c** showing the atomic numbering scheme**Fig. 2** Molecular structure of [Ta(OC₆HPh₂-2,6-Bu^t-3,5)₂Cl₃] **1e** showing the atomic numbering scheme

isostructural with previously reported [Ta(OC₆H₃Bu^t-2,6)₂Cl₃]¹² and [Nb(OC₆HPh₄-2,3,5,6)₂Cl₃]¹³ and contrast with the chloro-bridged, dimeric [M(OC₆H₃Prⁱ-2,6)₂Cl₃]₂ (M = Nb or Ta).¹⁴ The tris(2,6-diphenylphenoxide) [Ta(OC₆H₃Ph₂-2,6)₃Cl]₂ **2a** has also been previously reported by reaction of **1a** with 1 equivalent of LiOC₆H₃Ph₂-2,6 (Scheme 1).¹⁵ The reaction of trichloride **1a** and dichloride **2a** with LiCH₂SiMe₃ leads to the formation of the corresponding alkyls **4a** and **5a** (Scheme 2). The intermediate monochloride **3a** was isolated in good yield

Table 2 Selected bond distances (Å) and angles (°) for [Ta(OC₆HPh₂-2,6-Me₂-3,5)₂(CH₂SiMe₃)₃] **4c**

Molecule 1		Molecule 2	
Ta(1)–O(10)	1.89(1)	Ta(2)–O(20)	1.93(1)
Ta(1)–O(12)	1.90(1)	Ta(2)–O(22)	1.91(1)
Ta(1)–C(150)	2.10(2)	Ta(2)–C(250)	2.17(2)
Ta(1)–C(160)	2.16(2)	Ta(2)–C(260)	2.16(1)
Ta(1)–C(170)	2.13(1)	Ta(2)–C(270)	2.10(2)
O(10)–Ta(1)–O(12)	174.8(5)	O(20)–Ta(2)–O(22)	174.0(4)
O(10)–Ta(1)–C(150)	93.7(5)	O(20)–Ta(2)–C(250)	88.6(5)
O(10)–Ta(1)–C(160)	88.3(5)	O(20)–Ta(2)–C(260)	92.3(5)
O(10)–Ta(1)–C(170)	91.2(5)	O(20)–Ta(2)–C(270)	89.6(5)
O(12)–Ta(1)–C(150)	88.0(5)	O(22)–Ta(2)–C(250)	85.4(5)
O(12)–Ta(1)–C(160)	86.7(5)	O(22)–Ta(2)–C(260)	91.3(5)
O(12)–Ta(1)–C(170)	92.3(5)	O(22)–Ta(2)–C(270)	92.6(6)
C(150)–Ta(1)–C(160)	125.7(6)	C(250)–Ta(2)–C(260)	120.1(6)
C(150)–Ta(1)–C(170)	120.1(6)	C(250)–Ta(2)–C(270)	118.8(6)
C(160)–Ta(1)–C(170)	114.2(6)	C(260)–Ta(2)–C(270)	121.1(6)
Ta(1)–O(10)–C(101)	177.5(11)	Ta(2)–O(20)–C(201)	174.5(11)
Ta(1)–O(12)–C(121)	165.4(11)	Ta(2)–O(22)–C(221)	164.3(12)
Ta(1)–C(150)–Si(15)	130.7(9)	Ta(2)–C(250)–Si(25)	132.6(9)
Ta(1)–C(160)–Si(16)	139.9(9)	Ta(2)–C(260)–Si(26)	126.4(8)
Ta(1)–C(170)–Si(17)	130.4(9)	Ta(2)–C(270)–Si(27)	127.7(8)

Table 3 Selected bond distances (Å) and angles (°) for [Ta(OC₆HPh₂-2,6-Prⁱ-3,5)₂(CH₂SiMe₃)₃] **4d**

Ta–O(10)	1.922(3)	Ta–C(160)	2.130(5)
Ta–O(12)	1.908(3)	Ta–C(170)	2.121(5)
Ta–C(150)	2.180(5)		
O(10)–Ta–O(12)	168.9(1)	C(150)–Ta–C(170)	110.3(2)
O(10)–Ta–C(150)	85.6(2)	C(160)–Ta–C(170)	119.1(2)
O(10)–Ta–C(160)	93.0(2)	Ta–O(10)–C(101)	151.7(3)
O(10)–Ta–C(170)	92.2(2)	Ta–O(12)–C(121)	150.3(3)
O(12)–Ta–C(150)	84.7(2)	Ta–C(150)–Si(15)	142.5(3)
O(12)–Ta–C(160)	89.1(2)	Ta–C(160)–Si(16)	128.3(3)
O(12)–Ta–C(170)	96.3(2)	Ta–C(170)–Si(17)	132.4(3)
C(150)–Ta–C(160)	130.6(2)		

Table 4 Selected bond distances (Å) and angles (°) for [Ta(OC₆H₃Ph₂-2,6)₃(CH₂SiMe₃)₂] **5a**

Ta–O(3)	1.930(3)	Ta–O(4)	1.918(3)
Ta–O(5)	1.912(3)	Ta–C(11)	2.090(6)
Ta–C(21)	2.122(5)		
O(3)–Ta–O(4)	87.7(1)	O(3)–Ta–O(5)	174.3(1)
O(3)–Ta–C(11)	91.6(2)	O(3)–Ta–C(21)	87.1(2)
O(4)–Ta–O(5)	89.2(1)	O(4)–Ta–C(11)	117.6(2)
O(4)–Ta–C(21)	131.6(2)	O(5)–Ta–C(11)	94.1(2)
O(5)–Ta–C(21)	91.5(1)	Ta–O(3)–C(31)	152.8(3)
Ta–O(4)–C(41)	152.4(3)	Ta–O(5)–C(51)	159.1(3)
Ta–C(11)–Si(1)	139.2(3)	Ta–C(21)–Si(2)	128.5(3)

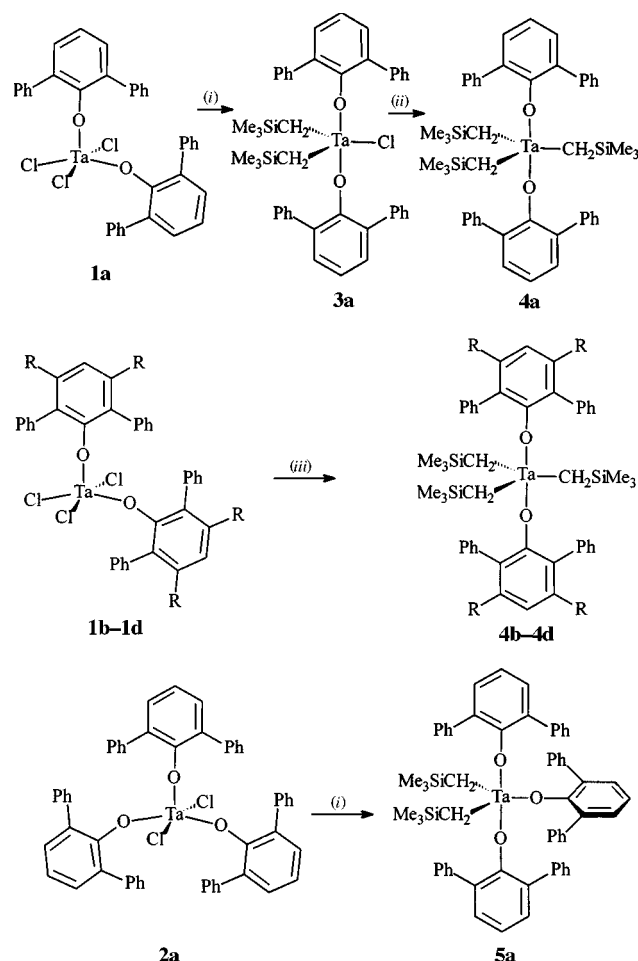
by treating **1a** with only 2 equivalents of either ClMgCH₂SiMe₃ or LiCH₂SiMe₃. The *meta*-phenyl, -methyl and -isopropyl substituted trichlorides **1b–1d** react similarly with LiCH₂SiMe₃ to produce **4b–4d** (Scheme 2). The solid-state structures of **4c**, **4d** and **5a** show trigonal-bipyramidal geometries with axial aryloxy groups (Tables 2–4; Figs. 3–5).

The ¹H NMR spectra of the compounds **4a–4d** are highly informative. In **4a** the methylene protons Ta–CH₂SiMe₃ appear as a sharp singlet at δ –0.05. As the *meta* substituent is changed this signal moves progressively upfield and broadens, appearing in the ambient spectrum of the *meta*-isopropyl derivative as a hump above the baseline at δ –0.59 (Table 5). An important characteristic of terminal, non-metallated *ortho*-aryl phenoxide ligands is the diamagnetic shielding of protons of ligands that are in close proximity to the central co-ordination sphere.¹⁵ In the solid-state structures of **4c** and **4d** (Figs. 3 and 4) the orientation of the two axial aryloxy ligands is such that

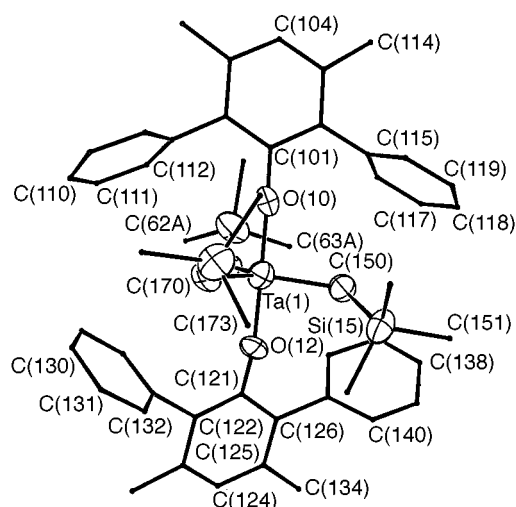
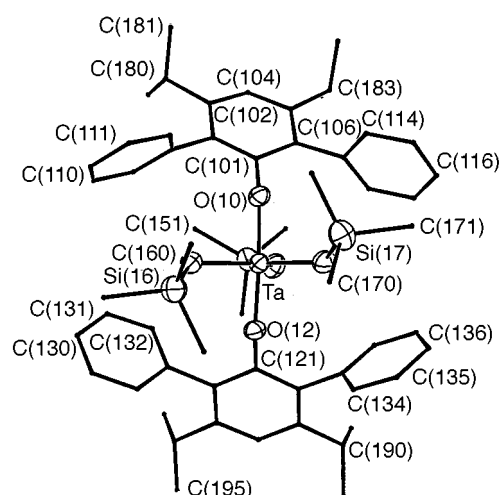
Table 5 Selected NMR spectroscopic data (C₆D₆)

Compound	I δ(OH)	4 δ(TaCH ₂ SiMe ₃)		6 δ(Ta=CHSiMe ₃)	δ(TaCH ₂ SiMe ₃)	δ(Ta=CHSiMe ₃)	¹ J(¹³ C– ¹ H)/Hz
		25 °C	–80 °C				
a	5.39	–0.15	0.96, –0.59	8.56	–0.05	237.0	116.4
b	5.24	–0.32	0.77, –0.82	7.85	–0.49	234.4	113.5
c	4.72	–0.49	0.69, –1.02	*	–0.83	229.2	113.6
d	4.58	–0.59	0.60, –1.20	*	–0.87	227.8	111.1
e	4.33	—	—	6.55	–1.19	227.3	113.1

* Obscured by aromatic signals.



the alkyl ligands occupy two distinct environments. Two of the CH₂SiMe₃ ligands are directly below the aryloxy phenyl rings while the third alkyl in the trigonal plane lies away from the aryloxy ligands. Upon cooling to sub-ambient temperatures the spectra of **4a–4d** show collapse and separation of the Ta–CH₂ signal into two resonances in the ratio 1:2, with the larger resonance being upfield (Table 5). The position of the low field resonance is typical of Ta–CH₂SiMe₃ groups in the absence of any unusual ligand effects. The dramatically upfield shifted resonance can be ascribed to the two alkyl groups below the aryloxy phenyl rings. The chemical shift difference between these two signals attests to the diamagnetic shielding caused by these aryloxy ligands. Based upon these data we conclude that restricted rotation of the aryloxy ligands takes place on the NMR time-scale. The coalescence temperature for the exchange is raised as the bulk of the *meta* substituent increases. This can be rationalized by arguing that substitution at the *meta* position decreases the conformational flexibility of the ligand and leads to an increase in effective steric bulk (see below).

**Fig. 3** Molecular structure of [Ta(OC₆HPh₂-2,6-Me₂-3,5)₂(CH₂SiMe₃)₃] **4c** showing the atomic numbering scheme**Fig. 4** Molecular structure of [Ta(OC₆HPh₂-2,6-Pr¹-3,5)₂(CH₂SiMe₃)₃] **4d** showing the atomic numbering scheme

Treatment of *meta-tert*-butyl-substituted **1e** with LiCH₂SiMe₃ (3 equivalents) led to the formation of the alkylidene complex **6e** along with 1 equivalent of SiMe₄ (Scheme 3). This reactivity is identical to that documented for the corresponding 2,6-di-*tert*-butylphenoxide complex.¹¹ It has been well documented that bulky ancillary ligation can expedite α -hydrogen abstraction processes.¹⁰ This result, therefore, indicates that the *tert*-butyl substituent has dramatically increased the steric bulk of the ligand over its isopropyl counterpart. The analogous alkylidene compounds **6a–6d** can, however, be generated by photolysis of tris(alkyls) **4a–4d** in hydrocarbon solution (Scheme 3). Monitoring the reaction in C₆D₆ solution by ¹H NMR spectroscopy shows the photo-reaction is highly efficient at producing the alkylidene and

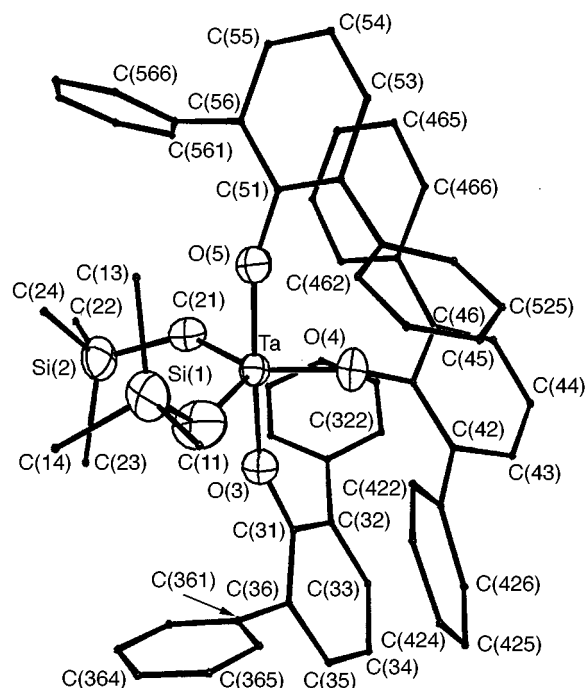
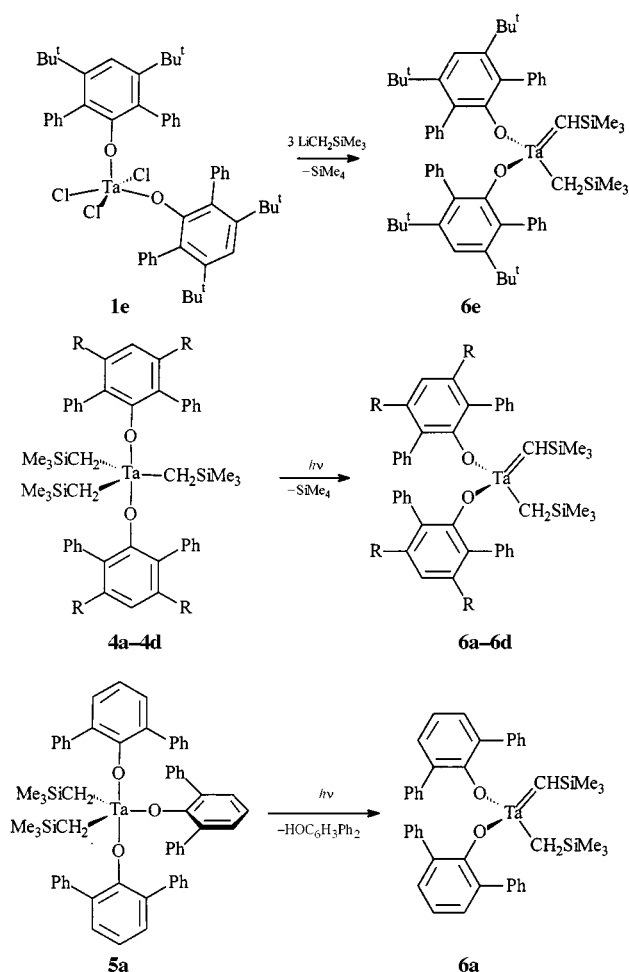
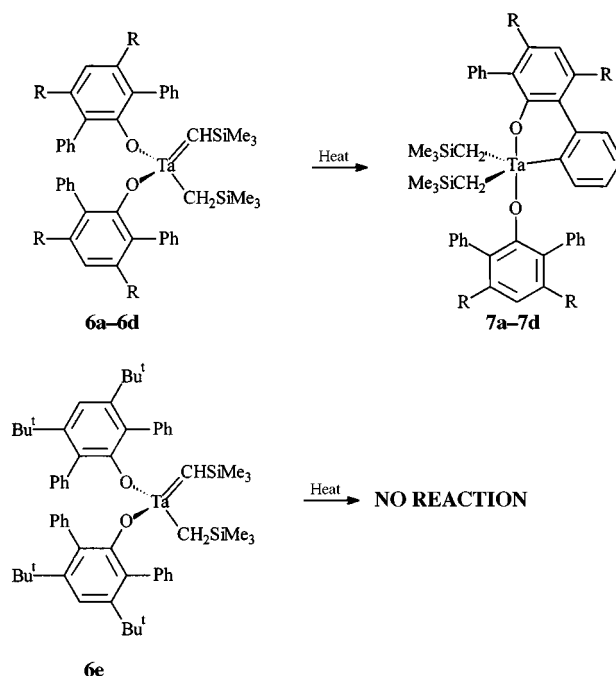


Fig. 5 Molecular structure of $[\text{Ta}(\text{OC}_6\text{H}_3\text{Ph}_2\text{-2,6})_3(\text{CH}_2\text{SiMe}_3)_2]$ **5a** showing the atomic numbering scheme



Scheme 3

1 equivalent of SiMe_4 . Previous studies by our group have shown that the generation of the tantalum alkylidene function by photochemical α -hydrogen abstraction occurs by excitation into a ligand-to-metal charge-transfer band



Scheme 4

within the d^0 -alkyl precursor to generate an incipient alkyl radical.¹¹

A surprising observation is that photolysis of the tris(aryl-oxide) **5a** leads to the alkylidene **6a** with elimination (1H NMR spectroscopy) of 1 equivalent of 2,6-diphenylphenol (Scheme 3). The mixture of **6a** and 2,6-diphenylphenol does not thermally convert back to the tris(aryl-oxide) **5a**. This represents a rare example of the formation of an early d-block metal alkylidene by α -hydrogenation abstraction by a heteroatom-bound leaving group. This result implies that photolysis of **5a** leads to selective breaking of a tantalum–phenoxide bond (presumably the equatorial ligand, Fig. 5) over a tantalum–alkyl bond leading either to an incipient or solvent trapped 2,6-diphenylphenoxide radical which abstracts the α -hydrogen atom leading to **6a**.

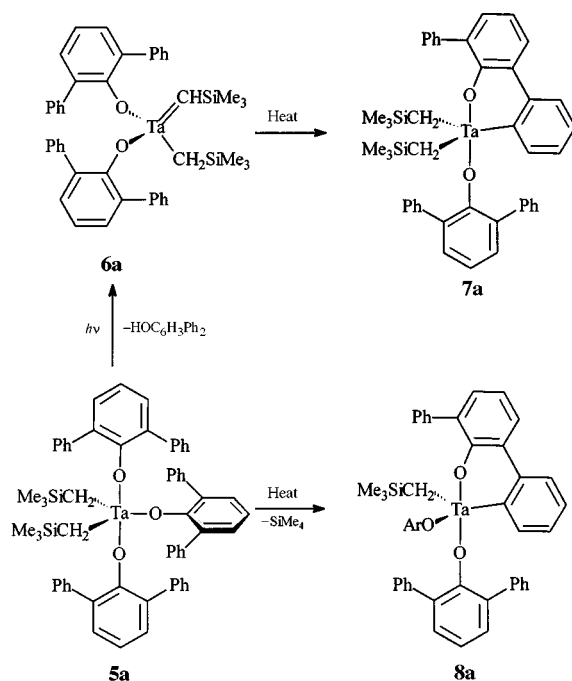
The alkylidene compounds **6a–6e** exhibit dramatically different thermal stabilities in benzene and toluene solution. The simple 2,6-diphenylphenoxide **6a** converts over hours in C_6D_6 or $\text{C}_6\text{D}_5\text{CD}_3$ solution at ambient temperatures to produce the cyclometallation product **7a**. Analogous monocyclometallated compounds **7b–7d** can also be formed from the *meta*-phenyl-, -methyl and -isopropyl derivatives **6b–6d** (Scheme 4). In this case, however, ring closure occurs very slowly at ambient temperatures but heating **6b–6d** in C_6D_6 or $\text{C}_6\text{D}_5\text{CD}_3$ solution shows the clean formation of **7b–7d** at progressively slower rates as the bulk of the *meta* substituent increases (see mechanistic study below). In contrast, *tert*-butyl-substituted **6e** fails to form any cyclometallated derivative upon extended thermolysis. Solutions of **6e** in $\text{C}_6\text{D}_5\text{CD}_3$ show little change (1H NMR) upon heating at 105 °C for weeks. This is a remarkable thermal stability for an early-transition-metal alkylidene compound.

Monocyclometallated compounds can also be generated by thermolysis of the alkyls **4a–4d** and **5a**. The tris(alkyls) **4a–4d** produce the metallated compounds **7a–7d** that were also obtained *via* photogenerated **6a–6d**. These reactions require high temperatures and were found to also produce secondary thermal products, which were not isolated, but are presumably bis-cyclometallated derivatives as previously reported for related compounds.^{3,7a} In contrast, bis(alkyl) **5a** generated the complex **8a** and 1 equivalent of SiMe_4 . Hence, different monocyclometallated complexes are generated *via* photochemical or thermal pathways for **5a** (Scheme 5).

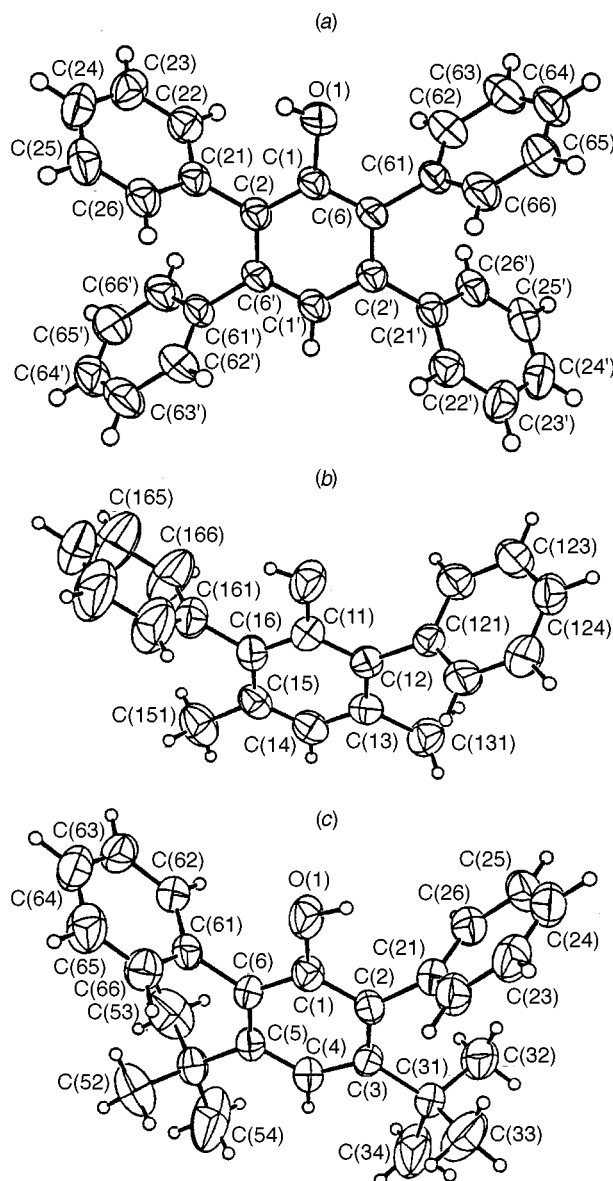
Table 6 Values of dihedral angle (τ) for selected 2,6-diphenylphenoxides containing 3,5-substituents (R)

R	Compound	τ	Ref.
Ph	1b $\text{HOC}_6\text{HPh}_4\text{-2,3,5,6}$	69, 75	*
	$[\text{Nb}(\text{OC}_6\text{HPh}_4\text{-2,3,5,6})_2\text{Cl}_3]$	60, 61	13
	$[\text{W}(\text{OC}_6\text{HPh}_4\text{-2,3,5,6})_2(\text{NPh})_2]$	60, 58, 56, 55	8(a)
Me	1c $\text{HOC}_6\text{HPh}_2\text{-2,6-Me}_2\text{-3,5}$	67, 89	*
	1c $[\text{Ta}(\text{OC}_6\text{HPh}_2\text{-2,6-Me}_2\text{-3,5})_2\text{Cl}_3]$	61, 72, 74, 88	*
	4c $[\text{Ta}(\text{OC}_6\text{HPh}_2\text{-2,6-Me}_2\text{-3,5})_2\text{-}(\text{CH}_2\text{SiMe}_3)_3]$	66, 71, 79, 80	*
			*
Pr^i	4d $[\text{Ta}(\text{OC}_6\text{HPh}_2\text{-2,6-Pr}^i_2\text{-3,5})_2\text{-}(\text{CH}_2\text{SiMe}_3)_3]$	70, 78, 82, 83	*
			*
Bu^t	1e $\text{HOC}_6\text{HPh}_2\text{-2,6-Bu}^t_2\text{-3,5}$	87, 89	*
	1e $[\text{Ta}(\text{OC}_6\text{HPh}_2\text{-2,6-Bu}^t_2\text{-3,5})_2\text{Cl}_3]$	76, 81, 81, 84	*

* This work.

**Scheme 5****Structural analysis and spectroscopic probes of conformational flexibility**

The parent aryl alcohols 2-phenylphenol¹⁶ and 2,6-diphenylphenol¹⁷ have previously been subjected to structural study. Early interest in the *ortho*-arylphenols stemmed from the spectroscopic detection of O–H π hydrogen bonding.¹⁸ We have subjected the ligand precursors 2,3,5,6-tetraphenylphenol **1b**, 2,6-diphenyl-3,5-dimethylphenol **1c** and 2,6-diphenyl-3,5-di-*tert*-butylphenol **1e** to single crystal X-ray diffraction analysis (Fig. 6). All three molecules are found to be monomeric in the solid state with the hydroxyl proton bent towards one of the *ortho*-phenyl rings. For the purposes of this study the most important feature of these structures is not the parameters for the π interaction, but the ground-state conformation of the aryl rings. It can be seen (Table 6) that the introduction of *meta* substituents leads to larger dihedral angles (τ) between the *ortho*-phenyl and phenoxy rings. There is now an extensive amount of literature on metal derivatives of the 2,6-diphenylphenoxide ligand. The data derived from the Cambridge Structural Database combined with the parameters obtained in this study for **5a** can be analyzed as shown in Fig. 7. It can be seen that the value of τ for this ligand is clustered between 40–55° with an average value of 49°. In only a few cases is the angle

**Fig. 6** Molecular structures of $\text{HOC}_6\text{HPh}_4\text{-2,3,5,6}$ **1b**, $\text{HOC}_6\text{H}_3\text{Ph}_2\text{-2,6-Me}_2\text{-3,5}$ **1c** and $\text{HOC}_6\text{H}_3\text{Ph}_2\text{-2,6-Bu}^t_2\text{-3,5}$ **1e**

greater than 75°. Introduction of *meta* substituents leads to a distinct increase in the values of τ (Table 6) with the *tert*-butyl substituent forcing the *ortho*-phenyl ring very close to perpendicular to the phenoxide ring.

Analysis of the NMR spectroscopic data for the organometallic compounds obtained in this study shows a correlation between the chemical shift of alkyl and alkylidene α -protons and the nature of the *meta* substituents. The size of these shifts (Table 5) cannot be accounted for by electronic effects transmitted through the phenoxide backbone. The upfield shifting of alkylidene α -CH resonances has been shown to take place when an *agostic* interaction is present.¹⁹ The values of the $^1J(^{13}\text{C}\text{--}^1\text{H})$ coupling constant show little evidence for such an interaction (Table 5).²⁰ Instead we ascribe the progressive upfield shifting of these resonances to the average conformation adopted by the *ortho*-phenyl rings in solution. As the bulk of the *meta* substituent increases it forces the phenyl rings perpendicular and restricts their conformational flexibility. This leads to greater diamagnetic shielding of protons in close proximity to the metal and provides a spectroscopic tool for judging the steric impact of the substituents. Furthermore, the conformational rigidity of the 3,5-di-*tert*-butylphenoxide ligand results in it functioning as a more bulky ligand than the other analogues.

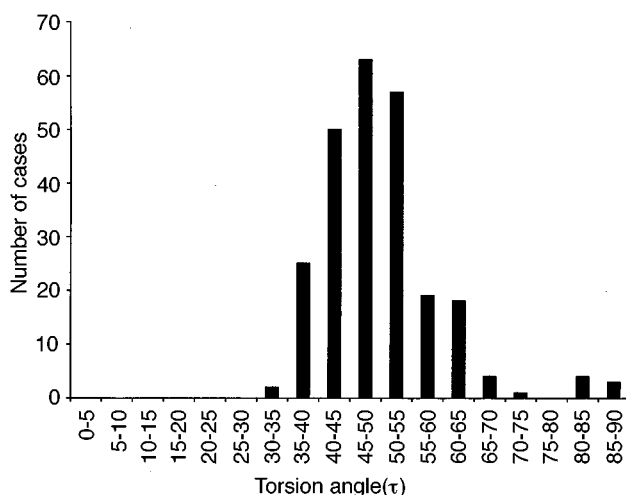


Fig. 7 Distribution of torsion angles (τ) for structurally characterized 2,6-diphenylphenoxide derivatives of transition metals. Data obtained from the Cambridge Crystallographic Database

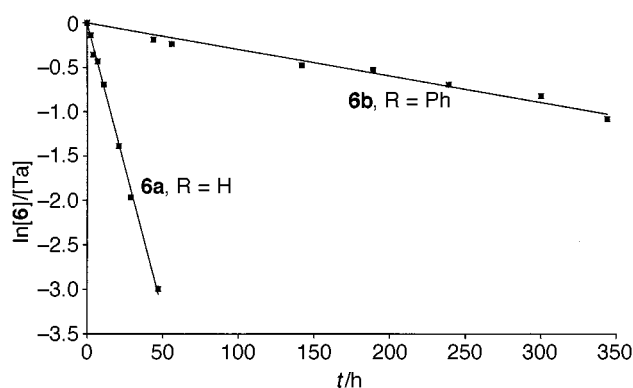
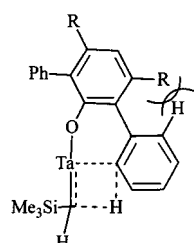


Fig. 8 First-order plots of the disappearance of photogenerated **6a** and **6b** at 20 °C in C_6D_6 solvent



Scheme 6

Mechanistic considerations

The conversion of the tantalum alkylidene compounds **6a–6d** into the monocyclometallated derivatives **7a–7d** represents the intramolecular addition of an aromatic C–H bond across the tantalum–alkylidene double bond.²¹ The intramolecular activation of aliphatic C–H bonds by tantalum alkylidenes and by other metal alkylidene and alkylidyne bonds is well predated.²² More recently the intermolecular activation of arene C–H bonds by early d-block metal alkylidenes has been reported.²³ There are also similarities with the activation of C–H bonds by early d-block metal imido functional groups.²⁴ Based upon previous mechanistic work, it is reasonable to propose a transition state for the reaction involving a four-center, four-electron transition state in which the hydrogen of the arene C–H bond is transferred to the alkylidene α -carbon simultaneous with the formation of the new Ta–C (aryl) bond (Scheme 6). The transition state requires the *ortho*-phenyl ring to rotate almost coplanar with the central phenoxy ring in order for the C–H bond to be brought into close proximity to the

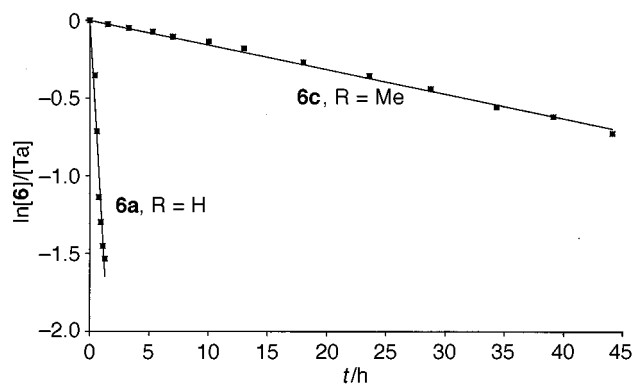


Fig. 9 First-order plots of the disappearance of photogenerated **6a** and **6c** at 58 °C in C_6D_6 solvent

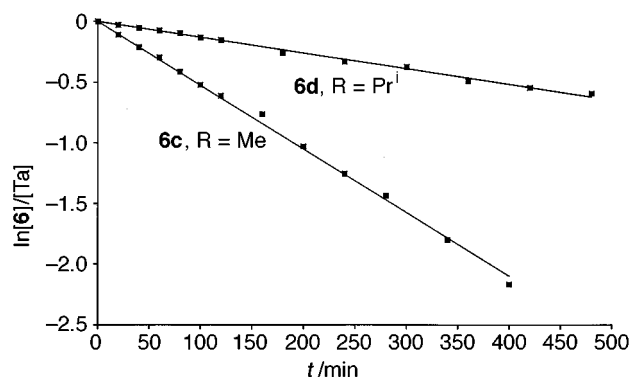


Fig. 10 First-order plots of the disappearance of photogenerated **6c** and **6d** at 97 °C in $C_6D_5CD_3$ solvent

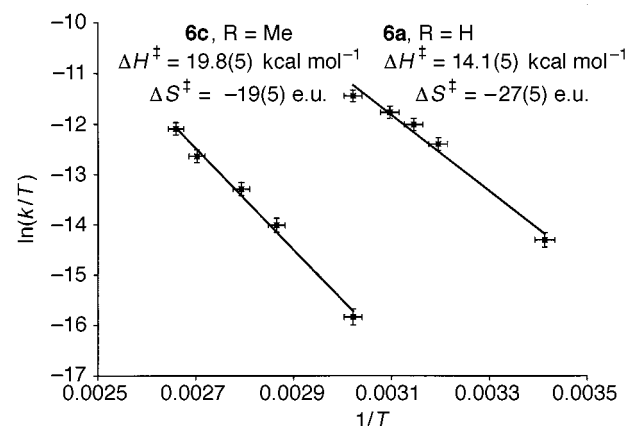


Fig. 11 Plots of $\ln(k/T)$ vs. $1/T$ for the disappearance of photogenerated **6a** and **6c** (cal = 4.184 J, e.u. = 4.184 J K⁻¹ mol⁻¹)

tantalum alkylidene group. Kinetic studies of the reactions in C_6D_6 or $C_6D_5CD_3$ solution show clean first-order decay of **6a–6d** when monitored by ¹H NMR spectroscopy. These studies show the *meta*-phenyl substituent inhibits ring closure by a factor of 22 at 20 °C (Fig. 8) while the *meta*-methyl compound cyclometallates 90 times slower than the parent molecule **6a** at 58 °C (Fig. 9). At 97 °C the isopropyl compound reacts four times slower than the methyl derivative (Fig. 10). These data (with the caveat that they were obtained at different temperatures, see below) leads us to specify that *meta*-phenyl, -methyl and -isopropyl substituents retard cyclometallation of adjacent phenyl rings in **6** by a factor of 20, 90 and 360 respectively in this temperature regime.

Activation parameters obtained for the cyclometallation of the unsubstituted and *meta*-methyl compounds (**6a** and **6c**, Fig. 11, Table 7) show both reactions have a moderately large negative entropy of activation. The intramolecular activation of C–H bonds by σ -bond metathesis^{25,26} or by addition to

Table 7 First-order rate constants measured for the conversion of **6** to **7**

Reaction	$T/^{\circ}\text{C}$	$10^4 k/\text{s}^{-1}$
6a \longrightarrow 4a	20	2.0
6a \longrightarrow 7a	40	13
6a \longrightarrow 7a	45	20
6a \longrightarrow 7a	50	25
6a \longrightarrow 7a	58	36
6b \longrightarrow 7b	20	0.083
6c \longrightarrow 7c	58	0.40
6c \longrightarrow 7c	76	3.0
6c \longrightarrow 7c	85	6.1
6c \longrightarrow 7c	97	9.2
6c \longrightarrow 7c	103	21
6d \longrightarrow 7d	97	2.2

unsaturated functional groups²⁴ typically display such negative values of ΔS^{\ddagger} (highly ordered transition state). The enthalpic increase observed on introducing the *meta*-methyl substituent accounts for the rate drop of approximately 90 at 58 °C. This increase in ΔH^{\ddagger} can be ascribed to the extra energy needed to rotate the phenyl ring approximately coplanar with the phenoxide ring due to clash of the *ortho*-proton with the methyl substituent. It should, however, be pointed out that the non-parallel nature of the lines in Fig. 11 means that the relative rates of cyclometallation are temperature dependent. Furthermore the activation parameters imply an isokinetic temperature of 800 K, *i.e.* above this temperature the *meta*-methyl compound will cyclometallate faster than the unsubstituted derivative.

Experimental

All operations were carried out under a dry nitrogen atmosphere in a Vacuum Atmospheres Dri-Lab or by standard Schlenk techniques. The hydrocarbon solvents were distilled from sodium benzophenone and stored under nitrogen until use. 2,6-Diphenylphenol **1a** is commercially available (Aldrich), 2,3,5,6-tetraphenylphenol **1b**,²⁵ 2,6-diphenyl-3,5-di-*tert*-butylphenol **1e**,⁹ 2,6-dimethyl-4-hepten-3-one, [Ta(OC₆H₃Ph₂-2,6)₂Cl₃]¹⁵ **1a** and [Ta(OC₆H₃Ph₂-2,6)₃Cl₂]¹⁵ **2a** were made by previously reported procedures. Literature preparation of 2,6-diphenyl-3,5-dimethylphenol has previously been reported in a preliminary fashion,²⁷ additional details are included here. Photolysis experiments were carried out using an Ace Hanovia 450 W Hg lamp cooled by a water condenser. The ¹H and ¹³C NMR spectra were recorded on a Varian Associates Gemini-200 spectrometer and referenced to protio impurities of commercial C₆D₆ or C₆D₅CD₃. Variable-temperature ¹H NMR spectra were recorded on a broad band Gemini XL 200A spectrometer and referenced to the protio impurities in C₆D₅CD₃. The X-ray diffraction studies were carried out 'in house' at Purdue University.

2,6-Diphenyl-3,5-dimethylcyclohex-2-enone

A 100 cm³ round bottom flask was charged with pent-3-en-2-one (65% pure, 5.0 g, 39 mmol), 1,3-diphenylpropan-2-one (10.7 g, 51 mmol), dry methanol (75 cm³) and NaOMe (5.4 g, 0.11 mol). Large white crystals formed from the dark orange solution upon standing overnight at room temperature. The supernatant was decanted, the solid washed with a small portion of ice-cold methanol and dried *in vacuo* to yield 2,6-diphenyl-3,5-dimethylcyclohex-2-enone (4.3 g, 16 mmol, 41%) as a white solid. High resolution mass spectrum: Found: 276.1516. Calc. for C₂₀H₂₀O: 276.1514. ¹H NMR (CDCl₃, 30 °C): δ 7.1–7.6 (m, 10 H, aromatics), 3.40 (d, 1 H), 2.5 (m, 3 H), 1.93 (s, 3 H), 1.01 (d, 3 H). ¹³C NMR (CDCl₃, 30 °C): δ 197.6, 155.2, 138.7, 137.3, 135.7, 128.95, 128.9, 128.0, 127.6, 126.7, 126.4, 60.8, 40.4, 35.0, 22.5, 20.5. M.p. = 129–130 °C.

2,6-Diphenyl-3,5-dimethylphenol **1c**

A 250 cm³ round bottom flask was charged with 2,6-diphenyl-3,5-dimethylcyclohex-2-enone (4.3 g, 39 mmol) and 10% palladium on activated carbon (0.5 g). The reaction mixture was heated until the evolution of hydrogen gas ceased. The cooled solid was extracted with methylene chloride, filtered and the solvent removed under reduced pressure to yield 3.6 g of 2,6-diphenyl-3,5-dimethylphenol (13 mmol, 87%) as a white solid. High resolution mass spectrum: Found: 274.1359. Calc. for C₂₀H₁₈O: 274.1358. ¹H NMR (CDCl₃, 30 °C): δ_{H} 7.2–7.7 (m, 10 H), 6.88 (s, 1 H), 4.78 (s, 1 H), 2.16 (s, 6 H). ¹³C NMR (CDCl₃, 30 °C): δ 149.9, 136.2, 130.2, 128.8, 128.3, 127.5, 125.8, 123.3, 20.3. M.p. = 197–199 °C.

2,6-Diphenyl-3,5-diisopropylcyclohex-2-enone

To a 250 cm³ round bottom flask containing sodium (1.0 g, 43 mmol) dissolved in methanol (50 cm³) was added 1,3-diphenylacetone (5.0 g, 36 mmol) and 2,6-dimethyl-4-hepten-3-one (8.3 g, 40 mmol). The solution was stirred at room temperature for 1 h, a further 4.5 g of sodium (200 mmol) in methanol (50 cm³) were added and the solution refluxed for 12 h. The solid that formed upon cooling in an ice bath was collected by filtration, washed with ice-cold methanol and dried *in vacuo* for 2 h to yield 6.5 g of 2,6-diphenyl-3,5-diisopropylcyclohex-2-enone (56% yield) as a white solid. ¹H NMR (CDCl₃, 30 °C): δ 7.0–7.4 (m, 10 H, aromatics), 3.58 (d, 1 H), 2.77 (spt, 1 H), 2.49 (m, 1 H), 2.31 (m, 2 H), 1.63 (spt of d, 1 H), 0.8–1.1 (overlapping doublets, 12 H). ¹³C NMR (CDCl₃, 30 °C): δ 198.9 (C=O), 164.0, 139.0, 136.4, 136.1, 129.6, 128.8, 128.2, 127.8, 126.8, 126.4, 57.7, 45.8, 32.4, 27.9, 23.1, 20.8, 20.4, 20.2, 16.0. M.p. = 124–125 °C.

2,6-Diphenyl-3,5-diisopropylphenol **1d**

An identical procedure to that used for **1c** utilizing 2,6-diphenyl-3,5-diisopropylcyclohex-2-enone yielded 2,6-diphenyl-3,5-diisopropylphenol as white crystals. ¹H NMR (CDCl₃, 30 °C): δ 7.3–7.5 (m, 10 H, aromatics), 6.98 (s, 1 H, *para*-H), 4.58 (s, 1 H, OH), 2.80 (spt, 2 H), 1.17 (d, 12 H). ¹³C NMR (CDCl₃, 30 °C): δ 149.2, 147.2, 136.4, 130.5, 128.7, 127.5, 124.6, 113.7, 30.1, 24.1.

[Ta(OC₆HPh₄-2,3,5,6)₂Cl₃] **1b**

A two-neck, 250 cm³ flask equipped with a nitrogen adaptor and reflux condenser was filled with [TaCl₅] (9.0 g, 26.0 mmol) suspended in benzene (100 cm³). While being stirred, 2,3,5,6-tetraphenylphenol (21.8 g, 55.0 mmol) was slowly added portionwise to the pale yellow solution under a nitrogen flush. The orange-yellow solution was periodically placed under a vacuum to remove HCl, then refluxed for 2 h, cooled and the solvent removed *in vacuo* to give a yellow powder. The crude solid was washed with a small portion of pentane and dried to yield 25.0 g of [Ta(OC₆HPh₄-2,3,5,6)₂Cl₃] (88% yield) (Found: C, 66.12; H, 4.06; Cl, 10.03. Calc. for C₆₀H₄₂Cl₃O₂Ta: C, 66.59; H, 3.91; Cl, 9.83%).

[Ta(OC₆HPh₂-2,6-Me₂-3,5)₂Cl₃] **1c**

A 250 cm³ two-neck flask was charged with [TaCl₅] (2.77 g, 8.0 mmol) in benzene (100 cm³) under a nitrogen flush. Solid 2,6-diphenyl-3,5-dimethylphenol (4.4 g, 16.0 mmol) was added in portions over a 30 min period. Stirring was continued for 2 h at room temperature and the solvent was then removed *in vacuo*. The yellow solid was redissolved in a minimum amount of hot toluene–benzene and allowed to stand overnight. The orange crystals which formed were washed with a small amount of hexane and dried *in vacuo* to yield 1.8 g (3.0 mmol, 38%) of [Ta(OC₆HPh₂-2,6-Me₂-3,5)₂Cl₃] (Found: C, 40.74; H, 2.88; Cl, 22.77. Calc. for C₂₀H₁₇Cl₃O₂Ta: C, 40.30; H, 2.88; Cl, 23.78%). The supernatant was layered with hexane to induce the formation of yellow crystals of [Ta(OC₆HPh₂-2,6-Me₂-3,5)₂Cl₃]

which were washed with a small portion of pentane and dried *in vacuo*. Yield: 2.4 g (2.9 mmol, 36%) (Found: C, 59.40; H, 4.31; Cl, 11.68. Calc. for $C_{43}H_{37}Cl_3OTa \cdot 0.5C_6H_6$: C, 59.16; H, 4.27; Cl, 12.18%). 1H NMR (C_6D_6 , 30 °C): δ 7.0–7.3 (m, 20 H, aromatics), 6.72 (s, 2 H, *para*-H), 1.93 (s, 12 H, Me). ^{13}C NMR (C_6D_6 , 30 °C): δ 159.1 (TaOC), 136.5, 131.3, 130.7, 130.0, 129.1, 129.0, 128.1, 20.4 (Me).

[Ta(OC₆HPh₂-2,6-Prⁱ₂-3,5)₂Cl₃] **1d**

A 250 cm³ two-neck flask was charged with [TaCl₅] (1.20 g, 3.5 mmol) in benzene (100 cm³) under a nitrogen flush. With stirring, 3,5-diisopropyl-2,6-diphenylphenol (2.45 g, 7.1 mmol) was slowly added portionwise to the pale yellow solution under a nitrogen flush. The deep yellow-green solution was periodically placed under vacuum to remove HCl, then refluxed for 2 h, cooled and the solvent removed *in vacuo* to give a yellow powder. The crude solid was washed with a small portion of pentane and dried *in vacuo* for 2 h to yield 1.8 g of [Ta(OC₆HPh₂-2,6-Prⁱ₂-3,5)₂Cl₃] (55% yield). 1H NMR (C_6D_6 , 30 °C): δ 7.0–7.5 (m, 22 H, aromatics), 2.85 (spt, 4 H), 1.10 (d, 24 H). ^{13}C NMR (C_6D_6 , 30 °C): δ 158.9 (TaOC), 147.9, 136.3, 131.0, 130.2, 129.3, 128.2, 127.8, 119.5, 30.3, 24.2.

[Ta(OC₆HPh₂-2,6-Bu^t₂-3,5)₂Cl₃] **1e**

A 250 cm³ two-neck flask was charged with [TaCl₅] (2.40 g, 7.0 mmol) in benzene (50 cm³) under a nitrogen flush and 2,6-diphenyl-3,5-di-*tert*-butylphenol (6.0 g, 17 mmol) were then added portionwise over a 20 min period. After the addition was complete, the solution was refluxed for 6 h. After removing the solvent *in vacuo*, the crude solid was redissolved in a minimum amount of hot hexane and slowly cooled to produce large yellow crystals of [Ta(OC₆HPh₂-2,6-Bu^t₂-3,5)₂Cl₃]. These crystals were washed with a small amount of hexane and dried *in vacuo*. Yield: 1.5 g (21%) (Found: C, 62.81; H, 6.15; Cl, 10.03. Calc. for $C_{52}H_{58}Cl_3O_2Ta$: C, 63.43; H, 5.90; Cl, 10.21%). 1H NMR (C_6D_6 , 30 °C): δ 7.68 (s, 2 H, *para*-H), 7.16–7.25 (m, 20 H, aromatics), 1.17 (s, 36 H, Bu^t). ^{13}C NMR (C_6D_6 , 30 °C): δ 162.5 (TaOC), 148.4, 138.6, 132.8, 131.3, 129.3, 128.2, 123.6, 38.1 (CMe₃), 33.5 (CMe₃).

[Ta(OC₆H₃Ph₂-2,6)₂Cl(CH₂SiMe₃)₂] **3a**

Method (a). To a suspension of [Ta(OC₆H₃Ph₂-2,6)₂Cl₃] **1a** (10 g, 12.85 mmol) in benzene (50 cm³) was added LiCH₂SiMe₃ (2.54 g, 26.98 mmol). The reaction was stirred for 30 min, filtered to remove the lithium chloride salts and dried *in vacuo* to give **3a** an off-white solid which was washed with hexane and dried *in vacuo*. Yield: 3.50 g (31%).

Method (b). To a suspension of [Ta(OC₆H₃Ph₂-2,6)₂Cl₃] **1a** (34.72 g, 44.63 mmol) in benzene (100 cm³) was added slowly dropwise at 0 °C a solution of ClMgCH₂SiMe₃ (147 mmol) in diethyl ether (150 cm³). Upon complete addition, the mixture was gradually warmed to room temperature and stirred for 16 h, filtered to remove the lithium chloride salts and dried *in vacuo* to give an off-white solid. Recrystallization of the resulting crude solid from toluene afforded colorless crystals of **3a** which were washed with hexane and dried *in vacuo*. Yield: 35.5 g (91%) (Found: C, 60.00; H, 5.47; Cl, 4.19. Calc. for $C_{44}H_{48}ClO_2Si_2Ta$: C, 59.96; H, 5.49; Cl, 4.02%). 1H NMR (C_6D_6 , 30 °C): δ 6.82–7.50 (m, 26 H, aromatics), 0.42 (s, 4 H, CH₂SiMe₃), –0.04 (s, 18 H, SiMe₃). ^{13}C NMR (C_6D_6 , 30 °C): δ 157.4 (TaOC), 123.5–140.6 (aromatics), 83.9 (TaCH₂SiMe₃), 2.61 (SiMe₃).

[Ta(OC₆H₃Ph₂-2,6)₂(CH₂SiMe₃)₂] **4a**

To a suspension of [Ta(OC₆H₃Ph₂-2,6)₂Cl₃] **1a** (0.99 g, 1.27 mmol) in benzene (10 cm³) was added LiCH₂SiMe₃ (0.37 g, 3.92

mmol). The reaction was stirred for 6 h, filtered to remove the lithium chloride and dried *in vacuo* to give an off-white solid. Recrystallization from toluene afforded colorless crystals of **4a** which were washed with hexane and dried *in vacuo*. Yield: 1.02 g (86%) (Found: C, 61.93; H, 6.35. Calc. for $C_{48}H_{59}O_2Si_3Ta$: C, 61.78; H, 6.37%). 1H NMR (C_6D_6 , 30 °C): δ 6.78–7.58 (m, 26 H, aromatics), 0.04 (s, 27 H, CH₂SiMe₃), –0.05 (s, 6 H, CH₂SiMe₃). ^{13}C NMR (C_6D_6 , 30 °C): δ 157.7 (TaOC), 122.3–141.6 (aromatics), 72.2 (TaCH₂SiMe₃), 3.84 (SiMe₃).

[Ta(OC₆HPh₄-2,3,5,6)₂(CH₂SiMe₃)₃] **4b**

To a suspension of [Ta(OC₆HPh₄-2,3,5,6)₂Cl₃] **1b** (5.0 g, 4.62 mmol) in benzene (20 cm³) was added LiCH₂SiMe₃ (1.35 g, 14.3 mmol). The reaction was stirred for 6 h, filtered to remove the lithium chloride salts and dried *in vacuo* to give **4b** as a light yellow solid which was washed with hexane and dried *in vacuo*. 1H NMR (C_6D_6 , 30 °C): δ 6.89–7.41 (m, 42 H, aromatics), 0.15 (s, 27 H, CH₂SiMe₃), –0.24 (br s, 6 H, CH₂SiMe₃). ^{13}C NMR (C_6D_6 , 30 °C): δ 158.3 (TaOC), 143.3–125.8 (aromatics), 72.3 (br, TaCH₂SiMe₃), 3.90 (SiMe₃).

[Ta(OC₆HPh₂-2,6-Me₂-3,5)₂(CH₂SiMe₃)₂] **4c**

A benzene solution (50 cm³) containing [Ta(OC₆HMe₂-3,5-Ph₂-2,6)₂Cl₃] **1c** (1.0 g, 1.2 mmol) was treated with LiCH₂SiMe₃ (0.4 g, 4.2 mmol) and the resulting mixture was stirred at room temperature for 2 h during which time a fine white precipitate of LiCl formed. The solution was filtered and the solvent removed *in vacuo*. The crude white solid was dissolved in a minimum amount of pentane, cooled slowly to –20 °C and the resulting white crystals of **4c** dried *in vacuo*. Yield: 1.0 g (85%) suitable for X-ray diffraction (Found: C, 62.78; H, 7.09. Calc. for $C_{52}H_{67}O_2Si_3Ta$: C, 63.13; H, 6.83%). 1H NMR (C_6D_6 , 30 °C): δ 7.00–7.35 (m, 20 H, aromatics), 6.74 (s, 2 H, *para*-H), 1.87 (s, 12 H, *meta*-Me), 0.10 (s, 27 H, CH₂SiMe₃), –0.43 (s, 6 H, CH₂SiMe₃). ^{13}C NMR (C_6D_6 , 30 °C): δ 158.1 (TaOC), 70.0 (TaCH₂SiMe₃), 4.0 (CH₂SiMe₃), 140.1, 137.2, 131.9, 131.6, 129.2, 127.3, 126.0.

[Ta(OC₆HPh₂-2,6-Prⁱ₂-3,5)₂(CH₂SiMe₃)₃] **4d**

A benzene solution (50 cm³) containing [Ta(OC₆HPh₂-2,6-Prⁱ₂-3,5)₂Cl₃] **1d** (0.60 g, 0.60 mmol) was treated with LiCH₂SiMe₃ (0.25 g, 2.0 mmol). After 2 h the solution was filtered and the solvent removed *in vacuo*. The crude white solid was dissolved in toluene and layered with pentane to induce the formation of colorless blocks of [Ta(OC₆HPh₂-2,6-Prⁱ₂-3,5)₂(CH₂SiMe₃)₃] **4d** (yield = 0.44 g, 70%) that were suitable for an X-ray diffraction study. 1H NMR (C_6D_6 , 30 °C): δ 7.0–7.5 (m, 22 H, aromatics), 2.64 (spt, 4 H), 1.14 (d, 24 H), 0.09 (s, 27 H), –0.50 (br s, 6 H, TaCH₂SiMe₃). ^{13}C NMR (C_6D_6 , 30 °C): δ 157.7 (TaOC), 78.5 (TaCH₂SiMe₃), 4.1 (CH₂SiMe₃), 148.5, 139.7, 131.9, 130.4, 130.0, 128.9, 128.3, 116.1, 30.3, 24.4.

[Ta(OC₆H₃Ph₂-2,6)₃(CH₂SiMe₃)₂] **5a**

To a suspension of [Ta(OC₆H₃Ph₂-2,6)₃Cl₂] **2a** (1.12 g, 1.13 mmol) in benzene (10 cm³) was added dropwise a solution of LiCH₂SiMe₃ (0.26 g, 2.76 mmol) in benzene (8 cm³). The reaction was stirred for 18 h, filtered to remove the lithium chloride solids and dried *in vacuo* to give an off-white solid. Recrystallization from toluene afforded white crystals which were washed with hexane and dried *in vacuo*. Yield 0.94 g (76%). 1H NMR (C_6D_6 , 30 °C): δ 6.35–7.50 (m, 39 H, aromatics), 0.82 (s, 4 H, CH₂SiMe₃), –0.15 (s, 18 H, CH₂SiMe₃). ^{13}C NMR (C_6D_6 , 30 °C): δ 157.8 (TaOC), 122.2–142.2 (aromatics), 82.8 (TaCH₂SiMe₃), 3.37 (SiMe₃).

[Ta(OC₆H₃Ph₂-2,6)₂(=CHSiMe₃)(CH₂SiMe₃)₂] **6a**

A saturated C_6D_6 solution of [Ta(OC₆H₃Ph₂-2,6)₂(CH₂SiMe₃)₃]

4a in a 5 mm NMR tube was placed 5 cm away from a 450 W Ace Hanovia medium-pressure Hg lamp housed in a water-cooled quartz jacket. The tube was cooled in water while being photolyzed for 45 min to produce a solution and the product characterized using NMR spectroscopy. ^1H NMR (C_6D_6 , 30 °C): δ 8.56 (s, 1 H, Ta=CH), 6.86–7.45 (m, 26 H, aromatics), 0.07 (s, 9 H, CH_2SiMe_3), 0.06 (s, 9 H, CH_2SiMe_3), –0.05 (s, 2 H, CH_2SiMe_3). ^{13}C NMR (C_6D_6 , 30 °C): δ 237.0 [Ta=CHSiMe₃], $^1J(^{13}\text{C}-^1\text{H}) = 116.4$ Hz], 157.3 (TaOC), 52.6 (TaCH₂SiMe₃), 2.06 (SiMe₃), 2.00 (SiMe₃).

[Ta(OC₆HPh₂-2,6-R₂-3,5)₂(=CHSiMe₃)(CH₂SiMe₃)] **6 (R = Ph b, Me c or Prⁱ d)**

These compounds were obtained by a procedure identical to that used for **6a**.

[Ta(OC₆HPh₄-2,3,5,6)₂(=CHSiMe₃)(CH₂SiMe₃)] **6b. ^1H NMR (C_6D_6 , 30 °C): δ 7.85 (s, 1 H, Ta=CH), 6.91–7.36 (m, 42 H, aromatics), 0.12 (s, 9 H, CH_2SiMe_3), 0.07 (s, 9 H, CH_2SiMe_3), –0.49 (s, 2 H, CH_2SiMe_3). ^{13}C NMR (C_6D_6 , 30 °C): δ 234.4 [Ta=CHSiMe₃], $^1J(^{13}\text{C}-^1\text{H}) = 113.5$ Hz], 158.7 (TaOC), 51.7 (TaCHSiMe₃), 3.68 (SiMe₃), 2.52 (SiMe₃).**

[Ta(OC₆HPh₂-2,6-Me₂-3,5)₂(=CHSiMe₃)(CH₂SiMe₃)] **6c. ^1H NMR (C_6D_6 , 30 °C): δ 6.90–7.45 (m, 21 H, Ta=CH plus aromatics), 6.66 (s, 2 H, *para*-H), 2.01 (s, 12 H, *meta*-Me), 0.10 (s, 9 H, CH_2SiMe_3), 0.02 (s, 9 H, CH_2SiMe_3), –0.83 (s, 2 H, CH_2SiMe_3). ^{13}C NMR (C_6D_6 , 30 °C): δ 229.2 [Ta=CHSiMe₃], $^1J(^{13}\text{C}-^1\text{H}) = 113.6$ Hz], 158.1 (TaOC), 48.3 (TaCH₂SiMe₃), 22.5 (*meta*-Me), 3.36 (SiMe₃), 2.63 (SiMe₃).**

[Ta(OC₆HPh₂-2,6-Prⁱ₂-3,5)₂(=CHSiMe₃)(CH₂SiMe₃)] **6d. ^1H NMR (C_6D_6 , 30 °C): δ 6.9–7.5 (m, 22 H, aromatics including alkylidene proton), 3.04 (spt, 4 H), 1.1–1.3 (m, 24 H), 0.22 (s, 9 H, SiMe₃), 0.03 (s, 9 H, SiMe₃), –0.87 (br s, 2 H, TaCH₂SiMe₃). ^{13}C NMR (C_6D_6 , 30 °C): δ 227.8 [Ta=CHSiMe₃], $^1J(^{13}\text{C}-^1\text{H}) = 111.1$ Hz], 157.0 (TaOC), 47.6 (TaCH₂SiMe₃), 4.0 (SiMe₃), 3.4 (SiMe₃), 147.2, 138.1, 130.6, 129.0, 127.8, 127.3, 116.0, 30.6, 24.4.**

[Ta(OC₆HPh₂-2,6-Bu^t₂-3,5)₂(=CHSiMe₃)(CH₂SiMe₃)] **6e**

A benzene solution (50 cm³) containing [Ta(OCHPh₂-2,6-Bu^t₂-3,5)₂Cl₃] (0.4 g, 0.4 mmol) was treated with 3 equivalents of LiCH₂SiMe₃ (0.11 g, 1.2 mmol) and stirred at room temperature for 2 h during which time a fine white precipitate of LiCl formed. The solution was filtered to remove the LiCl and the solvent removed *in vacuo*. The extremely soluble yellow product **6e** (3.0 g, 75% yield) was spectroscopically characterized. ^1H NMR (C_6D_6 , 30 °C): δ 7.63 (s, 2 H, *para*-H), 6.8–7.4 (m, 20 H, aromatics), 6.55 (s, 1 H, Ta=CH), 1.33 (s, 9 H, =CHSiMe₃), 1.28 (s, 36 H, Bu^t), 0.09 (s, 9 H, CH_2SiMe_3), –1.19 (s, 2 H, CH_2SiMe_3). ^{13}C NMR (C_6D_6 , 30 °C): δ 227.3 [Ta=CHSiMe₃], $^1J(^{13}\text{C}-^1\text{H}) = 113.1$ Hz], 159.9 (TaOC), 47.8 (TaCH₂SiMe₃), 37.8 (CMe), 33.5 (CMe₃), 3.9 (SiMe₃), 2.6 (SiMe₃), 140.1, 134.0, 132.2, 130.2, 119.8, 119.6.

[Ta(OC₆H₃Ph₂-2,6)(OC₆H₃Ph- η^1 -C₆H₄)(CH₂SiMe₃)₂] **7a**

The formation of the monocyclometallated compound **7a** was accomplished by thermolysis of C_6D_6 solutions of [Ta(OC₆H₃Ph₂-2,6)₂(CH₂SiMe₃)₃] **4a** in an oil bath at elevated temperatures (*e.g.* 90 °C). The kinetics of conversion of [Ta(OC₆H₃Ph₂-2,6)₂(=CHSiMe₃)(CH₂SiMe₃)] **6a** into **7a** was monitored in C_6D_6 solution by ^1H NMR spectroscopy. The product was not isolated in either case and was characterized by spectroscopic methods. ^1H NMR (C_6D_6 , 30 °C): δ 8.25 (d, 1 H), 7.99 (d, 1 H), 7.89 (d, 1 H), 7.69–6.83 (m, 19 H, aromatics), 0.90 (d, 2 H), –0.31 [d, 2 H, $^2J(^1\text{H}-^1\text{H}) = 11.8$ Hz, CH_2SiMe_3], –0.14 (s, 18 H, CH_2SiMe_3). ^{13}C NMR (C_6D_6 , 30 °C): δ 203.8 (TaC *ipso*), 76.5 (TaCH₂SiMe₃), 2.0 (CH₂SiMe₃).

[Ta(OC₆HPh₂-2,6-R₂-3,5)(OC₆HPh-2-R₂-3,5- η^1 -C₆H₄)(CH₂SiMe₃)₂] **7 (R = Ph b, Me c or Prⁱ d)**

These compounds were obtained by a procedure identical to that used for **7a**.

[Ta(OC₆HPh₄-2,3,5,6)(OC₆HPh₃- η^1 -C₆H₄)(CH₂SiMe₃)₂] **7b. ^1H NMR (C_6D_6 , 30 °C): δ 8.18 (d, 1 H), 6.70–7.60 (m, 40 H, aromatics), 0.77 (d, 2 H), –0.58 [d, 2 H, $^2J(^1\text{H}-^1\text{H}) = 11.9$ Hz, CH_2SiMe_3], –0.14 (s, 18 H, CH_2SiMe_3). ^{13}C NMR (C_6D_6 , 30 °C): δ 207.2 (TaC *ipso*), 76.0 (TaCH₂SiMe₃), 2.1 (CH₂SiMe₃).**

[Ta(OC₆HPh₂-2,6-Me₂-3,5)(OC₆HPh-2-Me₂-3,5- η^1 -C₆H₄)(CH₂SiMe₃)₂] **7c. ^1H NMR (C_6D_6 , 30 °C): δ 8.03 (d, 1 H), 7.67 (d, 2 H), 6.60–7.40 (m, 20 H, aromatics), 2.57 (s, 3 H), 1.90 (s, 6 H), 1.80 (s, 3 H, *meta*-Me), 0.77 (d, 2 H), 0.54 (d, 2 H), –0.81 [d, 2 H, $^2J(^1\text{H}-^1\text{H}) = 11.9$ Hz, CH_2SiMe_3], –0.18 (s, 18 H, CH_2SiMe_3). ^{13}C NMR (C_6D_6 , 30 °C): δ 205.5 (TaC *ipso*), 75.0 (TaCH₂SiMe₃), 21.3, 20.8, 20.7 (*meta*-Me), 2.1 (CH₂SiMe₃).**

[Ta(OC₆HPh₂-2,6-Prⁱ₂-3,5)(OC₆HPh-2-Prⁱ₂-3,5- η^1 -C₆H₄)(CH₂SiMe₃)₂] **7d. ^1H NMR (C_6D_6 , 30 °C): δ 8.16 (d, 1 H), 7.76 (d, 1 H), 6.80–7.50 (m, 20 H, aromatics), 3.85 (spt, 6 H), 2.86 (spt, 12 H), 2.64 (spt, 6 H, *meta*-Prⁱ), 1.46 (d, 6 H), 1.10–1.25 (m, 18 H), 0.60 (d, 2 H), –0.88 [d, 2 H, $^2J(^1\text{H}-^1\text{H}) = 12.0$ Hz, CH_2SiMe_3], –0.11 (s, 18 H, CH_2SiMe_3). ^{13}C NMR (C_6D_6 , 30 °C): δ 206.2 (TaC *ipso*), 74.4 (TaCH₂SiMe₃), 30.6, 25.9, 24.3 (*meta*-Prⁱ), 2.2 (CH₂SiMe₃).**

[Ta(OC₆H₃Ph₂-2,6)₂(OC₆H₃Ph- η^1 -C₆H₄)(CH₂SiMe₃)] **8a**

The formation of the monocyclometallated compound **8a** was accomplished by thermolysis of C_6D_6 solutions of [Ta(OC₆H₃Ph₂-2,6)₂(CH₂SiMe₃)₃] **5a** in an oil bath at elevated temperatures (*e.g.* 90 °C). ^1H NMR (C_6D_6 , 30 °C): δ 8.67 (d, 1 H, *o*-H on metallated phenyl ring), 8.07 (d, 1 H, *m*-H on metallated phenyl ring), 7.77 (d, 1 H, *m*-H on phenoxy ring), 7.70–6.32 (m, 29 H, aromatics), 0.60 (d, 1 H, CH_2SiMe_3), –0.03 (d, 1 H, CH_2SiMe_3), –0.07 (s, 9 H, SiMe₃). ^{13}C NMR (C_6D_6 , 30 °C): δ 201.4 (TaC *ipso*), 81.8 (TaCH₂), 1.50 (SiMe₃).

Crystallography

Crystal data for Ib. C₃₀H₂₂O, *M* = 398.51, monoclinic, space group *P* $\bar{1}$ (no. 2), *a* = 6.1569(8), *b* = 8.4102(5), *c* = 10.6947(13) Å, $\alpha = 99.764(7)^\circ$, $\beta = 92.094(11)^\circ$, $\gamma = 91.153(7)^\circ$, *T* = 296 K, *Z* = 1, *U* = 545.20(19) Å³, $\mu = 0.519$ mm^{–1}, number of reflections measured 2379, *R* = 0.057, *R'* = 0.143.

Crystal data for Ic. C₂₀H₁₈O, *M* = 274.37, monoclinic, space group *P*2₁/*n* (no. 14), *a* = 14.6884(11), *b* = 11.8059(14), *c* = 18.661(2) Å, $\beta = 104.321(7)^\circ$, *T* = 296 K, *Z* = 8, *U* = 3135.5(10) Å³, $\mu = 0.065$ mm^{–1}, number of reflections measured 5869, *R* = 0.048, *R'* = 0.122.

Crystal data for Ie. C₂₀H₃₀O, *M* = 358.53, monoclinic, space group *P*2₁/*c* (no. 14), *a* = 5.9464(7), *b* = 18.893(3), *c* = 19.0368(15) Å, $\beta = 97.113(8)^\circ$, *T* = 295 K, *Z* = 4, *U* = 2122.2(7) Å³, $\mu = 0.472$ mm^{–1}, number of reflections measured 4449, *R* = 0.059, *R'* = 0.145.

Crystal data for 1c·C₆H₆. C₄₆H₄₀Cl₃O₂Ta, *M* = 912.14, triclinic, space group *P* $\bar{1}$ (no. 2), *a* = 9.871(8), *b* = 11.618(7), *c* = 19.714(2) Å, $\alpha = 87.21(3)^\circ$, $\beta = 89.74(3)^\circ$, $\gamma = 64.90(5)^\circ$, *T* = 296 K, *Z* = 2, *U* = 2044(2) Å³, $\mu = 2.889$ mm^{–1}, number of reflections measured 8528, *R* = 0.039, *R'* = 0.047.

Crystal data for 1e·0.5C₆H₆. C₅₅H₆₁Cl₃O₂Ta, *M* = 1041.41, triclinic, space group *P* $\bar{1}$ (no. 2), *a* = 10.376(3), *b* = 13.1075(18), *c* = 19.798(3) Å, $\alpha = 72.391(12)^\circ$, $\beta = 89.39(2)^\circ$, $\gamma = 79.232(19)^\circ$,

$T = 297$ K, $Z = 2$, $U = 2518.3(12)$ Å³, $\mu = 2.354$ mm⁻¹, number of reflections measured 7103, $R = 0.024$, $R' = 0.032$.

Crystal data for 4c. C₅₂H₆₇O₂Si₃Ta, $M = 989.32$, monoclinic, space group $P2_1/c$ (no. 14), $a = 23.354(4)$, $b = 19.323(3)$, $c = 23.101(4)$ Å, $\beta = 102.474(15)^\circ$, $T = 296$ K, $Z = 8$, $U = 10\,178(5)$ Å³, $\mu = 4.925$ mm⁻¹, number of reflections measured 13 201, $R = 0.063$, $R' = 0.129$.

Crystal data for 4d. C₆₀H₈₃O₂Si₃Ta, $M = 1101.54$, monoclinic, space group $P2_1/c$ (no. 14), $a = 12.0448(12)$, $b = 14.399(2)$, $c = 34.848(4)$ Å, $\beta = 96.723(9)^\circ$, $T = 296$ K, $Z = 4$, $U = 6002(2)$ Å³, $\mu = 1.908$ mm⁻¹, number of reflections measured 7973, $R = 0.030$, $R' = 0.066$.

Crystal data for 5a. C₆₂H₆₁O₃Si₂Ta, $M = 1091.30$, triclinic, space group $P\bar{1}$ (no. 2), $a = 13.5220(19)$, $b = 13.6243(17)$, $c = 14.466(3)$ Å, $\alpha = 89.837(14)^\circ$, $\beta = 82.742(14)^\circ$, $\gamma = 81.403(11)^\circ$, $T = 295$ K, $Z = 2$, $U = 2613.7(11)$ Å³, $\mu = 4.648$ mm⁻¹, number of reflections 8672, $R = 0.035$, $R' = 0.041$.

CCDC reference number 186/611.

Acknowledgements

We thank the National Science Foundation (Grant CHE-9700269) for financial support of this research.

References

- 1 F. A. Cotton and G. Wilkinson, *Advanced Inorganic Chemistry*, Wiley-Interscience, New York, 5th edn., 1988.
- 2 *Activation and Functionalization of Alkanes*, ed. C. Hill, John Wiley and Sons, New York, 1989; *Selective Hydrocarbon Activation*, eds J. A. Davis, P. L. Watson, J. F. Liebman and A. Greenberg, VCH Publishers, Toledo, OH, 1989; A. E. Shilov, *Activation of Saturated Hydrocarbons by Transition Metal Complexes*, Reidel, Boston, 1984.
- 3 I. P. Rothwell, *Acc. Chem. Res.*, 1988, **21**, 153.
- 4 D. Rabinovich, R. Zelman and G. Parkin, *J. Am. Chem. Soc.*, 1990, **112**, 9632; 1992, **114**, 4611.
- 5 J. S. Yu, L. Felter, M. C. Potyen, J. R. Clark, V. M. Visciglio, P. E. Fanwick and I. P. Rothwell, *Organometallics*, 1996, **15**, 4443.
- 6 G. D. Smith, V. M. Visciglio, P. E. Fanwick and I. P. Rothwell, *Organometallics*, 1992, **11**, 1064.
- 7 (a) R. W. Chesnut, G. J. Gayatri, J. S. Yu, P. E. Fanwick and I. P. Rothwell, *Organometallics*, 1991, **10**, 321; (b) F. Lefebvre, M. Leconte, S. Pagano, A. Mutch and J.-M. Basset, *Polyhedron*, 1995, **14**, 3209.
- 8 (a) M. A. Lockwood, P. E. Fanwick, O. Eisenstein and I. P. Rothwell, *J. Am. Chem. Soc.*, 1996, **118**, 2762; (b) M. A. Lockwood, P. E. Fanwick and I. P. Rothwell, *Polyhedron*, 1995, **14**, 3363.
- 9 D. H. R. Barton, D. M. X. Donnelly, P. J. Guiry and J. H. Reibenspies, *J. Chem. Soc., Chem. Commun.*, 1990, 1110; D. H. R. Barton, N. Y. Bhatnagar, J.-C. Blazewski, B. Charpiot, J.-P. Finet, D. J. Lester, W. B. Motherwell, M. T. B. Papoula and S. P. Stanforth, *J. Chem. Soc., Perkin Trans. 1*, 1985, 2657.
- 10 R. R. Schrock, *Polyhedron*, 1995, **14**, 3177.
- 11 L. R. Chamberlain, I. P. Rothwell, K. Folting and J. C. Huffman, *J. Chem. Soc., Dalton Trans.*, 1987, 155; L. R. Chamberlain and I. P. Rothwell, *J. Chem. Soc., Dalton Trans.*, 1987, 163.
- 12 L. R. Chamberlain, I. P. Rothwell and J. C. Huffman, *Inorg. Chem.*, 1984, **23**, 2575.
- 13 M. A. Lockwood, M. C. Potyen, B. D. Steffey, P. E. Fanwick and I. P. Rothwell, *Polyhedron*, 1995, **14**, 3293.
- 14 J. R. Clark, A. L. Pulvirenti, P. E. Fanwick, M. Sigalis, O. Eisenstein and I. P. Rothwell, *Inorg. Chem.*, in the press.
- 15 R. W. Chesnut, L. D. Durfee, P. E. Fanwick, I. P. Rothwell, K. Folting and J. C. Huffman, *Polyhedron*, 1987, **6**, 2019.
- 16 M. Perrin, K. Bekkouch and A. Thozet, *Acta Crystallogr., Sect. C*, 1987, **43**, 2357.
- 17 K. Nakatsu, H. Yoshioka, K. Kunitomo, T. Kingasa and S. Ueki, *Acta Crystallogr., Sect. B*, 1978, **34**, 980.
- 18 M. Oki and H. Iwamura, *J. Am. Chem. Soc.*, 1967, **89**, 576; F. H. Allen, J. A. K. Howard, V. J. Hoy, G. R. Desiraju, D. S. Reddy and C. C. Wilson, *J. Am. Chem. Soc.*, 1996, **118**, 4081 and refs. therein.
- 19 M. Brookhart and M. L. H. Green, *J. Organomet. Chem.*, 1983, **250**, 395; M. Brookhart, M. L. H. Green and L. L. Wong, *Prog. Inorg. Chem.*, 1988, **36**, 1.
- 20 R. R. Schrock, R. T. DePue, J. Feldman, K. B. Yap, D. C. Yang, W. M. Davis, L. Y. Park, M. DiMare, M. Schofield, J. Anhaus, E. Walborsky, E. Evitt, C. Kruger and P. Betz, *Organometallics*, 1990, **9**, 2262.
- 21 I. P. Rothwell, in *Homogeneous Alkane Activation*, ed. C. G. Hill, Wiley, New York, 1989, pp. 151–195.
- 22 C. McDade, J. C. Green and J. E. Bercaw, *Organometallics*, 1982, **1**, 1629; A. R. Bulls, W. P. Schaefer, M. Serfas and J. E. Bercaw, *Organometallics*, 1987, **6**, 1219; L. R. Chamberlain, I. P. Rothwell and J. C. Huffman, *J. Am. Chem. Soc.*, 1986, **108**, 1502; J.-L. Couturier, C. Paillet, M. Leconte, J. M. Basset and K. Weiss, *Angew. Chem., Int. Ed. Engl.*, 1992, **31**, 628; K. C. Wallace, A. H. Liu, J. C. Dewan and R. R. Schrock, *J. Am. Chem. Soc.*, 1988, **110**, 4964; J. A. van Doorn, H. van der Heijden and A. G. Orpen, *Organometallics*, 1994, **13**, 4271.
- 23 H. van der Heijden and B. J. Hessen, *J. Chem. Soc., Chem. Commun.*, 1995, 145; M. P. Coles, V. C. Gibson, W. Clegg, M. R. J. Elsegood and P. A. Porrelli, *J. Chem. Soc., Chem. Commun.*, 1995, 145.
- 24 C. P. Schaller, C. C. Cummins and P. T. Wolczanski, *J. Am. Chem. Soc.*, 1996, **118**, 591.
- 25 P. Yates and J. R. Hyre, *J. Org. Chem.*, 1962, **27**, 4101; A. S. Hay and R. F. Clark, *Macromolecules*, 1970, **3**, 533; H. Yang and A. S. Hay, *Synthesis*, 1992, 467; D. E. Dana and A. S. Hay, *Synthesis*, 1982, 164.
- 26 D. H. Grayson and M. J. R. Tuite, *J. Chem. Soc., Perkin Trans. 1*, 1986, 2137.
- 27 A. Galan, A. J. Sutherland, P. Ballester and J. Rebek jun., *Tetrahedron Lett.*, 1994, **35**, 5359.

Received 4th April 1997; Paper 7/02325A